Supplement of Geochronology, 8, 351–371, 2026
https://doi.org/10.5194/gchron-8-351-2026-supplement

Supplement of

Atmospheric ^{10}Be from Talos Dome (East Antarctic) ice core records geomagnetic dipole intensity from 170 to 270 ka BP

Alexis Lamothe et al.

Correspondence to: Alexis Lamothe (alexis.lamothe@nju.edu.cn)

Figure S1: rolling averages

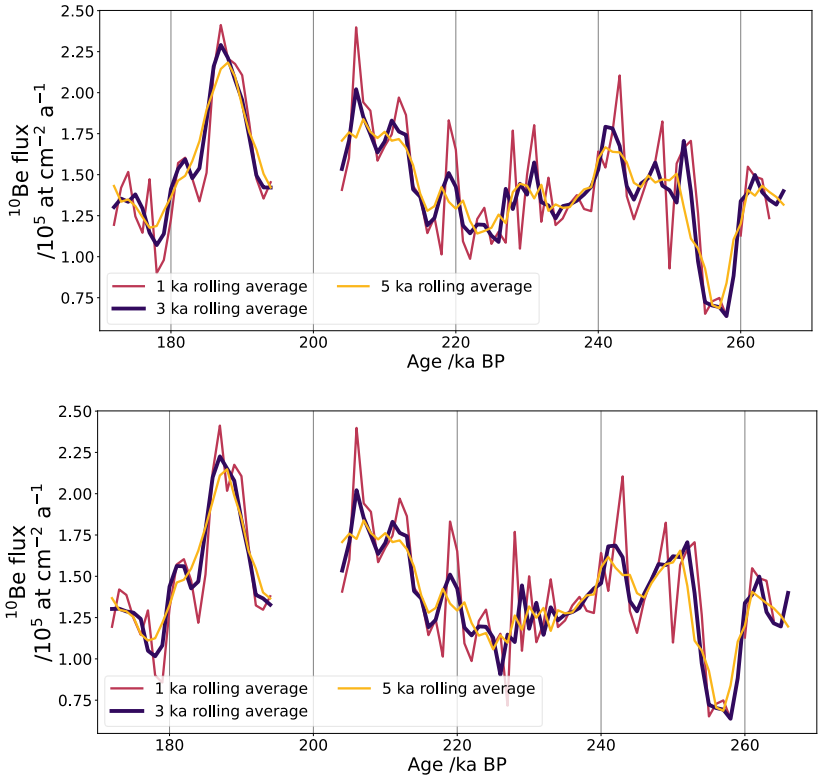

Comparison of three different rolling averages for ^{10}Be flux (/10^5 at cm^{-2} a^{-1}): with 1 ka (red), 3 ka (purple), 5 ka (orange)

Figure S2: median and mean averages

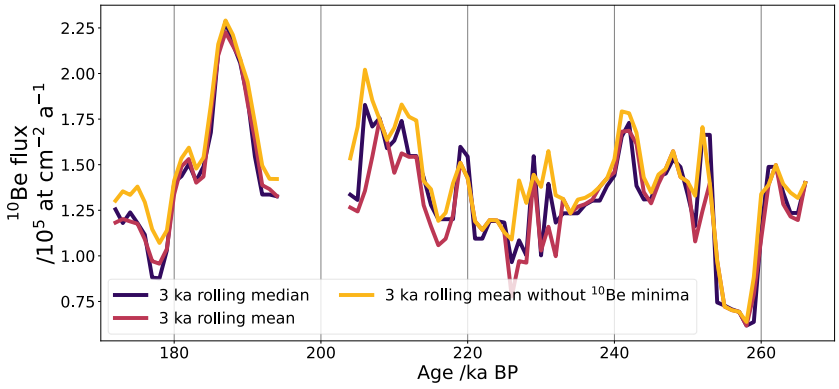

Comparison of three different rolling averages for ^{10}Be flux (/10^5 at cm^{-2} a^{-1}): with 3 ka rolling mean (red), 3 ka rolling median (purple), and a 3 ka rolling mean without the ^{10}Be minima (orange) in order to investigate the influence of minima on the flux variations.

Figure S3: comparison of sodium and ^{10}Be concentrations

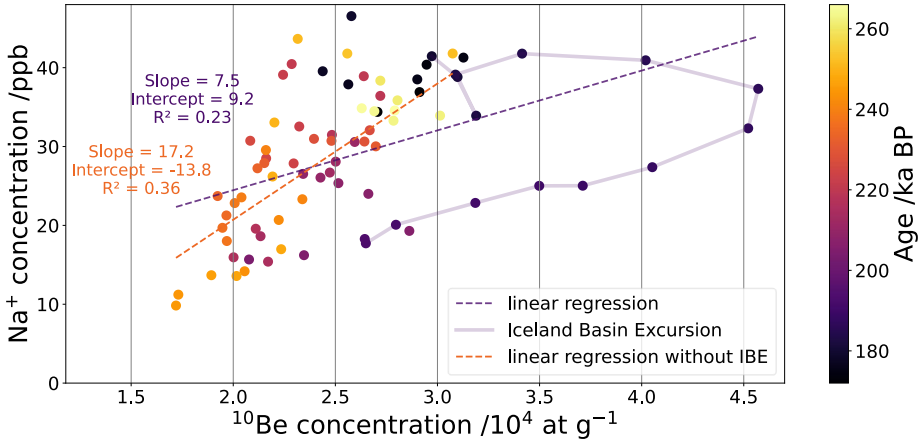

We investigate the contribution of climate variations on ^{10}Be concentration comparing Na^+ concentration (/ppb = ng g^{-1}) with ^{10}Be concentration (/10^4 at g^{-1}). Each dot represent one year mean average. The Iceland Basin excursions is easily identifiable (purple dots and curve) which affects the linear regression (dashed lines) between Na^+ and ^{10}Be concentrations.

Figure S4: correlation between MD05-2920 authigenic ^{10}Be/^{9}Be and TALDICE ^{10}Be flux records

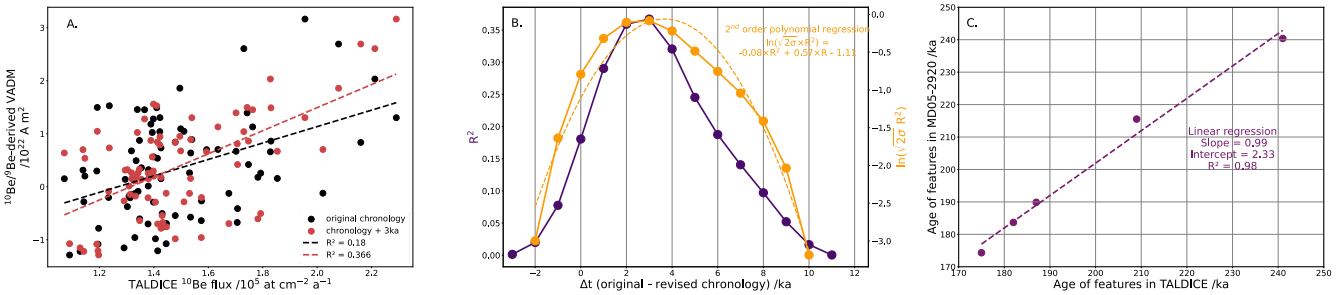

A. Comparison of the authigenic ^{10}Be/^{9}Be-based VADM (/10^{22} A m^2) from Simon et al., (2016) and TALDICE ^{10}Be flux (/10^5 at cm^{-2} a^{-1}) in the case of original oceanic chronology (black) or shifted 3 ka earlier (red). B. Cross-correlogram displaying R^2 (from the same variables as in Fig. A, purple) depending on fixed revision on the oceanic chronology (relative Δt = original – revised chronology, /ka). The correlation curve exhibits a Gaussian-like shape, with its maximum corresponding to the best temporal alignment between the two archives. The logarithm of the correlation ($\ln(\sqrt{2\sigma}R^2)$, orange dots) was fitted by a second-order polynomial (dashed orange line) to approximate a Gaussian function and determine the mean of the distribution (μ), representing the optimal offset between the records. C. Age-age relationship fort he same 5 distinguishable features in MD05-2920 (y axis) and TALDICE (x axis) as noted in Figure 5.

Table S1: list of studies reporting at the IBE, PFE alone, and IBE, PFE, and ME. The confusion between PFE and ME events are clarified in section 2.2.

Excursions recorded	Latitude	Longitude	Type of archive	Archive name	Source

IBE	43.48	-112.53	Volcano	site E at the Idaho National Engineering Laboratory INEL	Champion et al., 1988
PFE	43.78	-121.53	Sediment	Pringle falls	Herrero-Bervera et al.1989; 1994
IBE PFE ME	-1.64	159.22	Sediment	Ontong Java plateau ERDC 113p	Taux & Wu, 1990
IBE PFE ME	0	155.87	Sediment	Ontong Java plateau ERDC 89p	Taux & Wu, 1990
IBE	-3.09	-110.53	Sediment	ODP Sites 848	Valet & Meynadier, 1993
IBE	2.99	-110.5	Sediment	ODP Sites 851	Valet & Meynadier, 1993
IBE	1.01	136.96	Sediment	West Caroline Basin, western equatorial Pacific NP5	Yamazaki & Ioka, 1994
IBE	2	135	Sediment	West Caroline Basin, western equatorial Pacific NGC16	Yamazaki & Ioka, 1994
IBE	4.13	136.27	Sediment	West Caroline Basin, western equatorial Pacific NGC29	Yamazaki & Ioka, 1994
IBE	2	138.01	Sediment	West Caroline Basin, western equatorial Pacific NP7	Yamazaki & Ioka, 1994
IBE	3.8	141.48	Sediment	NP35	Yamazakia et al., 1995
IBE	1.22	160.57	Sediment	NGC36	Yamazakia et al., 1995
IBE	-14.99	175.17	Sediment	NGC38	Yamazakia et al., 1995
IBE	43.52	-30.4	Sediment	SU9008	Weeks et al., 1995
IBE	7.78	77.5	Sediment	KET82-51	Guyodo & Valet 1996
IBE	4.73	103.58	Sediment	DED87-07	Guyodo & Valet 1996
IBE	-2.55	91.33	Sediment	MD84-629	Guyodo & Valet 1996
IBE	-1.42	90.32	Sediment	MD85-668	Guyodo & Valet, 1996
IBE	-1.52	90.7	Sediment	MD85-669	Guyodo & Valet, 1996
IBE	-8.38	112.57	Sediment	MD85-674	Guyodo & Valet, 1996
IBE	9.9	121.53	Sediment	ODP 768A	Guyodo & Valet, 1996
IBE	10.75	121.57	Sediment	ODP 769B	Guyodo & Valet, 1996
IBE	39.37	-26.61	Sediment	SU-92-17	Lehman et al., 1996
IBE	37.79	-27.23	Sediment	SU-92-18	Lehman et al., 1996
IBE	37.3	-27.09	Sediment	SU-92-19	Lehman et al., 1996
IBE	44.68	168.23	Sediment	ODP Site 884	Roberts et al., 1997
IBE PFE ME	60.4	-23.6	Sediment	ODP Site 983	Channell et al., 1997; Knudsen et al., 2008; Christl et al., 2010
IBE	32.97	-76.28	Sediment	ODP Site 1061	ODP Leg 172 Scientific Party 1998
IBE PFE ME	32.98	-76.23	Sediment	ODP Site 1062	ODP Leg 172 Scientific Party 1998
IBE PFE ME	33.68	-57.62	Sediment	ODP Site 1063	ODP Leg 172 Scientific Party 1998; Knudsen et al., 2008; Christl et al., 2010; Channell et al., 2012
IBE	58.21	-48.37	Sediment	HU90-013-013P	Stoner et al., 1998
IBE	61.07	-24.02	Sediment	ODP Site 984	Channell et al., 1999
IBE	-19.7	246.5	Seafloor	East Pacific Rise (EPR)	Gee et al., 2000
IBE	-19.4	246.5	Seafloor	East Pacific Rise (EPR)	Gee et al., 2000
IBE PFE ME	53.6	108.3	Sediment	Lake Baikal	Oda et al., 2002; Demory et al., 2004
IBE	55.5	-14.7	Sediment	ODP Site 980	Channell & Raymo, 2003
IBE PFE ME	-40.9	9.9	Sediment	ODP Site 1089	Stoner et al., 2003
IBE PFE ME	37.8	-10.6	Sediment	MD95-2042	Thouveny et al., 2004; Carcaillet et al., 2004

IBE PFE ME	40.58	-9.87	Sediment	MD95-2040	Thouveny et al., 2004; Carcaillet et al., 2004
IBE PFE ME	62.67	-37.46	Sediment	ODP Site 919	Channell et al., 2006
IBE	58.93	-47.12	Sediment	MD99-2242	Laj et al., 2006
IBE	59.08	-31.47	Sediment	MD99-2247	Laj et al., 2006
IBE	19.58	117.63	Sediment	ODP Site 1145	Laj et al., 2006
IBE	16.45	116.27	Sediment	ODP Site 1146	Laj et al., 2006
IBE PFE ME	57.19	-47.13	Sediment	JPC-18	Evans et al., 2007
IBE PFE ME	47.6	-57.58	Sediment	JPC-19	Evans et al., 2007
IBE	32.77	130.28	Volcano	Unzen Volcano	Shibuya et al., 2007
IBE PFE ME	35.6	-106.75	Volcano	Albuquerque Volcanoes, NM	Singer et al., 2008
IBE	-50.2	-45.7	Sediment	IODP Site U1302/03	Channell et al., 2014
IBE	58.24	-45.64	Sediment	IODP Site U1306	Channell et al., 2014
IBE PFE ME	-10.53	147.22	Sediment	MD05-2930	Simon et al., 2016
IBE PFE ME	-2.51	144.32	Sediment	MD05-2920	Simon et al., 2016
IBE PFE ME	-0.103	-139.6	Sediment	KR0515-PC1	Yamazaki et al., 2008
IBE	-77.5	39.4	Ice core	Dome F	Horiuchi et al., 2016
IBE	2.77	-110.57	Sediment	ODP Site 851	Valet et al., 2020
IBE	39.08	-127.78	Sediment	ODP 1021	Valet et al., 2024

Table S2: TALDICE ^{10}Be concentrations over the last century

Top depth /m	Bottom depth /m	Mean depth /m	Top age /a CE	Bottom age /a CE	Mean age /a CE	^{10}Be conc. /at g^{-1}	Uncertainty of ^{10}Be conc. /at g^{-1}
4.5	5.0	4.8	1983.5	1980.7	1982.1	13193	575
5.0	5.5	5.2	1980.7	1977.8	1979.3	22939	714
5.5	6.0	5.7	1977.8	1975.0	1976.4	26440	831
6.0	6.5	6.3	1974.8	1971.6	1973.2	17023	531
6.5	7.0	6.8	1971.6	1968.9	1970.2	18894	670
7.0	7.5	7.3	1968.8	1965.6	1967.2	17675	630
7.5	8.0	7.8	1965.6	1962.9	1964.2	19577	612
8.0	8.5	8.2	1962.8	1959.9	1961.4	13802	453
8.5	9.0	8.7	1959.9	1956.8	1958.3	12714	398
9.0	9.5	9.3	1956.8	1953.7	1955.3	21421	668
9.5	10.0	9.7	1953.7	1950.7	1952.2	21526	672